Author's personal copy

Microelectronic Engineering 93 (2012) 19–26

Contents lists available at SciVerse ScienceDirect

Microelectronic Engineering

journal homepage: www.elsevier.com/locate/mee

Enhanced photo-patterning of polymer dielectrics via imprint lithography

Venmathy Rajarathinam, Sue Ann Bidstrup Allen, Paul A. Kohl *

School of Chemical & Biomolecular Engineering, Georgia Institute of Technology, 311 Ferst Drive, Atlanta, GA 30332-0100, United States

ARTICLE INFO

Article history:
Received 25 October 2010
Received in revised form 15 December 2011
Accepted 27 December 2011
Available online 4 January 2012

Keywords:
Imprint
Photolithography
Polynorbornene

ABSTRACT

An integrated photolithography and imprint lithography process has been developed to improve the patterning of photosensitive polymers in the fabrication of high aspect-ratio, polymer structures. In the photo-imprint process, a transparent stamp with surface relief structures was brought into contact with a photo-sensitive material. Temperature and pressure were applied to cause the photo-sensitive material to fill the mold, and UV light was then used to irradiate the polymer. The photo-imprint process advance was demonstrated on hollow-core structures. To develop high aspect-ratio, hollow-core pillars, a shallow photo-imprint stamp has been developed to physically displace material from the polymer core. Since the imprint stamp displaces material in the region of the feature, the effective film thickness is reduced compared to the bulk film. The reduction in film height decreased the effect of UV scattering in the core and also facilitated transport of the developer within the core. This photo-imprint lithography process is shown to be able to fabricate hollow core polymer pillars that exceed the optical-only resolution capabilities.

© 2012 Elsevier B.V. All rights reserved.

1. Introduction

Imprint lithography is a rapidly evolving field because of its potential as a next generation lithography technique that is economically viable and high resolution. There are many variations on the imprint process, but all require conformal replication of stamp topography to generate patterns. A stamp with a three dimensional pattern is pressed into a moldable material, and after the material replicates the pattern on the stamp, the material is hardened. Like other lithography techniques, imprint lithography requires precise *X–Y* stages, layer-to-layer alignment systems, and wafer handling equipment. However, the principal differentiator of imprint lithography from optical lithography techniques is that it is a contact patterning method. Its resolution is primarily limited by the resolution of the stamp and the pattern replica. Therefore, the main constraint of this technique is the ability to fabricate stamps of adequate spatial resolution and of sufficient durability since contact printing causes wear on the stamp. The quality of the pattern generated is limited by the capacity of a material to replicate the pattern, and the ability to separate the stamp and imprint material while retaining the imprinted shape.

Extensive research has been devoted over the past decade, to study the use of imprint lithography to enable manufacturing of semiconductor integrated circuits (ICs) at the nanometer scale. Chou et al. demonstrated the potential of thermal imprint lithography to fabricate sub 10 nm patterns [1–5]. Willson et al. have demonstrated patterned areas of high and low density, semi-dense and isolated lines to 20 nm [6].

Guo and coworkers developed a technique to integrate photolithography and imprint lithography [7]. In their technique, a hybrid mask was fabricated using an UV transparent substrate with metal pads to photo-pattern large features and protrusions to imprint nano-scale features [7]. Temperature and pressure were applied to cause the photosensitive imprint material to fill the mold, and UV light was then emitted to photo-pattern the polymer. Chemical selective removal of the residual layer was possible, and only small quantities of material had to be displaced.

Significant progress has been made with imprint lithography and the integrated photolithography and imprint lithography process to enable manufacturing of nanometer scale ICs. However, these ICs need to be connected to other components on a printed circuit board (PCB) to form electronic products. “Packaging” is defined as the bridge that connects the integrated circuit with other components on a system level [8]. Development of imprint lithography processes for advanced packaging applications could advance IC performance capabilities with high throughput and yield while maintaining low cost.

In this study, the integrated photolithography and imprint lithography process has been adapted to improve the photo-patterning of polymer dielectrics for high aspect ratio hollow structures. These structures are one example of the geometries that can be fabricated using the photo-imprint process for packaging applications. Many other structures can be imagined and are only limited by their utility. Particular focus has been placed on high aspect ratio hollow core pillars because a large application

* Corresponding author.
E-mail address: kohl@gatech.edu (P.A. Kohl).

0167-9317/$ - see front matter © 2012 Elsevier B.V. All rights reserved.
doi:10.1016/j.mee.2011.12.010

Author's personal copy

space exists for photosensitive, thick-film, high aspect ratio polymer dielectrics in microelectronics applications and MEMS including electroplating. However, high aspect ratio photo-processing of thick polymers is difficult with traditional photolithography. Thick films suffer from light scattering, resulting in poor resolution compared to thin films. Furthermore, structures with a narrow internal region are challenging to fabricate through photolithographic processes because the relative rate of transport of the developer in the core is slow compared to the rate of transport around the perimeter of the feature [9]. As a result, structures like hollow-core pillars require longer development times than solid pillars of comparable aspect ratios. At high aspect-ratios, delamination of the structure occurs before the core can be fully developed. Additionally, material limitations such as poor adhesion to the substrate can further exacerbate these challenges making this geometry difficult to fabricate.

The integrated photo-imprint process has been developed to mitigate the challenges of fabricating high aspect-ratio polymer structures using traditional photolithography. A shallow photo-imprint stamp shown in Fig. 1(b) was fabricated to physically move material in the polymer core. Since the imprint stamp displaces material in the area of the feature, the effective film thickness is reduced compared to the bulk film. The reduction in film height can lessen the diffractive and scattering effects in the core region by reducing the amount of material that needs to be developed away. Thus, the imprint assisted process described here can be used to enhance the photo-imaging capabilities of a photoresist or permanent dielectric material, regardless of what the imaging capabilities are of that system in a photo-lithography only process. The photo-imprint process was tested with two polynorbornene polymers, Avatrel 2000P and Avatrel 8000P (Promerus LLC, Brecksville, OH). This paper describes for the first time the use of a UV transparent and opaque stamp with physical relief features to imprint permanent dielectrics. The photo-imprint process provides a new tool in making physical relief features for packaging and MEMS devices.

Initial imprint tests were conducted with Avatrel 2000P a negative-tone, photosensitive, dielectric illustrated in Fig. 2. Avatrel 2000P is a random copolymer in which each of the seven-member norbornene rings on the backbone is functionalized with either alkyl or epoxide side groups. The properties of the Avatrel 2000P can be controlled by varying the ratio of alkyl-to-epoxide side groups. Avatrel 2000P is a photosensitive dielectric that is processed at 100 °C and cured at 160 °C. Cured films have a modulus of 1.0 GPa, a hardness of 0.04 GPa and a dielectric constant of 2.5. Avatrel 8000P, an aqueous base developed, photosensitive polymer, shown in Fig. 3, was also investigated as a high aspect ratio photo-imprintable material. Avatrel 8000P consists of a norbornene backbone with fluorinated alcohol groups which provide solubility in an aqueous base and carboxylic acid groups which provide cross-linking sites with added epoxy compounds. The polymer formulation is a mixture containing a multifunctional epoxy cross-linker, a photo-package, and an adhesion promoter. Avatrel 8000P has demonstrated a high contrast of 12.2 and the capability to produce high aspect ratio structures [9]. Cured films of Avatrel 8000P have a modulus of 2.9 GPa, a

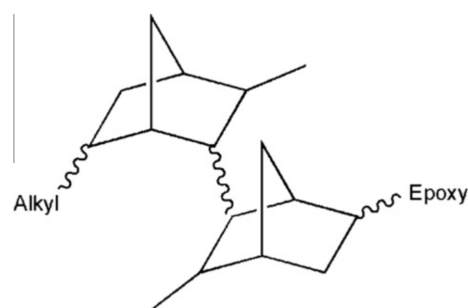

Fig. 2. Chemical structure of Avatrel 2000P.

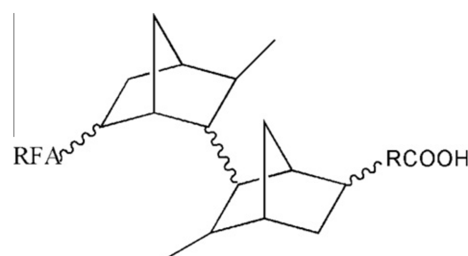

Fig. 3. Chemical structure of Avatrel 8000P.

hardness of 0.18 GPa and a dielectric constant of 3.9. Avatrel 2000P and Avatrel 8000P have different mechanical properties and photo-patterning capabilities, and the impact of their material properties on the photo-imprint lithography process is discussed.

2. Experimental

To create the photo-imprint stamp for patterning Avatrel 2000P, a glass substrate was sputtered with a full seed layer of chrome in the CVC DC Sputterer to a thickness of 1000 Å. The glass substrate was patterned with a Shipley photo-resist SC 1813. The SC 1813 was spin-coated to a thickness of 1.5 µm and soft baked at 90 °C for 3 min on a hotplate. The resist was photo-patterned at 100 mJ/cm^2 using the Karl Suss MA-6 Mask Aligner with a 350 W mercury lamp that exposes across the spectrum 230–400 nm. The sample was then developed in MF-319 (Shipley) to define the collar pattern. The chrome was patterned using chromium etchant CR-7 (Cyantek) and the SC 1813 was stripped in acetone. The sample was then sputtered with a full seed layer of Ti/Au/Ti (300 Å/3000 Å/300 Å) using the Unifilm Sputterer. The glass substrates were then patterned with AZ-4620 (AZ Electronic Materials) to pattern the molds for electroplating. The AZ-4620 was spin-coated to a thickness of 40 µm and soft baked at 100 °C for 30 min on a hotplate. The resist was photo-patterned at 1000 mJ/cm^2 using the Karl Suss MA-6 Mask Aligner. The sample was then developed in AZ-400K (AZ Electronic Materials) to define the mold for electroplating the stamp relief features. The titanium in the exposed region was wet etched back using buffered oxide etch

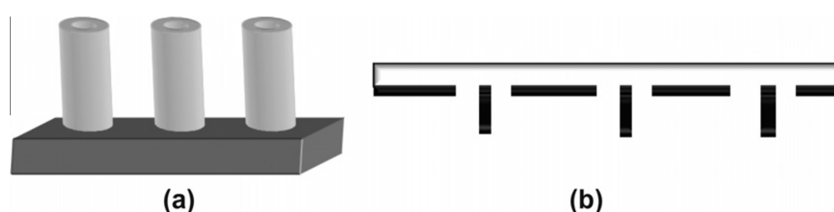

Fig. 1. (a) 3-D schematic of a high aspect ratio, hollow core pillar (b) 2-D schematic of photo-imprint stamp.

Author's personal copy

solution. Gold pillars were electroplated using a solution of 40 g/L $KAu(CN)_2$ and 100 g/L KH_2PO_4 at pH 7.2 and 40 °C. The AZ-4620 was stripped in acetone, and the titanium seed layers were etched back in buffered oxide etch solution. The gold seed layer was etched back in a 1:2:10–I_2:KI:H_2O solution. The photo-imprint stamp was coated with (3,3,3-trifluoropropyl)dimethylchlorosilane (Gelest) and then baked at 90 °C for 3 min.

To create the photo-imprint stamp for imprinting into Avatrel 8000P, a glass substrate was sputtered with a full seed layer of chrome in the CVC DC sputtering system to a thickness of 1000 Å. The glass substrate was patterned with NR-7 (Futurexx) spin-coated to a thickness of 2.5 μm and soft baked at 150 °C for 5 min on a hotplate. The resist was photo-patterned at 400 mJ/cm^2 using the Karl Suss MA-6 Mask Aligner. The sample was then post-exposure baked for 5 min at 100 °C and developed in RD-6 (Futurexx) to define the collar pattern. The chrome was patterned using chromium etchant CR-7 (Cyantek), and the NR-7 was stripped in acetone. The sample was then sputtered with a full seed layer of Ti/Cu/Ti (300 Å/3000 Å/300 Å) using the CVC DC Sputterer. The glass substrates were then patterned with NR-9 (Futurexx) to pattern the molds for electroplating. The NR-9 was spin-coated to a thickness of 10 μm and soft baked at 110 °C for 15 min on a hotplate. The resist was photo-patterned at 400 mJ/cm^2 using the Karl Suss MA-6 Mask Aligner. The sample was then post-exposure baked for 20 min at 110 °C and developed in RD-6 (Futurexx) to define the mold for electroplating. The titanium in the exposed region was wet etched back using buffered oxide etch solution, and copper pillars were electroplated. The NR-9 was stripped in acetone, and the titanium seed layers were etched back in buffered oxide etch solution. The copper seed layer was etched back in a 3% sulfuric acid and 3% hydrogen peroxide solution. The photo-imprint stamp was coated with Teflon AF and baked at 115 °C for 10 min to drive off solvent. The basic process flow for stamp fabrication for Avatrel 2000P and Avatrel 8000P is shown in Fig. 4.

Avatrel 2000P samples were spin-coated to varying thicknesses. The soft bake time and exposure doses were varied depending on the thickness of the material. The soft bakes were conducted on a hotplate at 100 °C, and post-exposure bakes were conducted in an oven at 100 °C for 20 min. Avatrel 2000P samples were developed in BIOACT EC-7R Defluxer (Petroferm) in an ultrasonic bath.

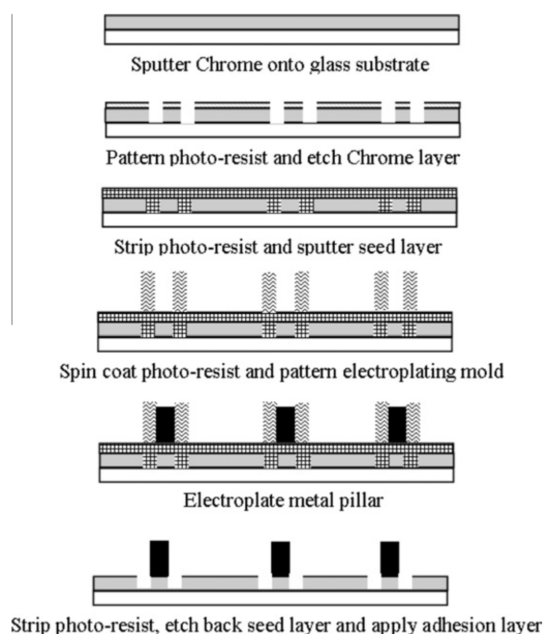

Fig. 4. Process steps for stamp fabrication using Avatrel 2000P and Avatrel 8000P.

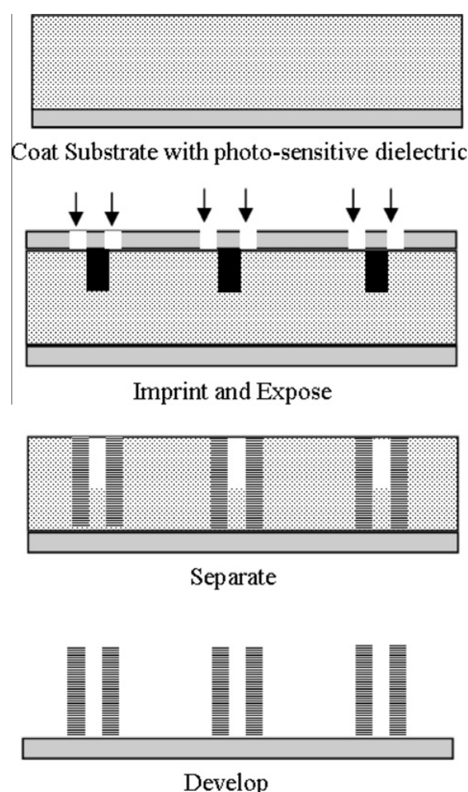

Fig. 5. Process flow for integrated photo-imprinting.

Avatrel 8000P samples received varying soft bake times and exposure doses depending on the thickness of the material. The soft bakes were conducted on a hotplate at 100 °C, and post-exposure bakes were conducted on a hotplate at 100 °C for 5 min. Avatrel 8000P was developed in MF-319 (Shipley) via puddle or ultrasonic bath.

All imprinting was conducted in the Obducat Imprint Lithography System, and exposures were conducted in the Karl Suss MA-6 Mask Aligner. The process flow for imprinting is shown in Fig. 5. The Hitachi 3500H was used to obtain scanning electron microscope (SEM) images of the processed films, but physically cross-sectioning the high aspect ratio polymer structures proved difficult due to the softness of the films. The Wyko non-contact profilometer was used as a non-destructive technique to obtain height profiles on the samples and to characterize the size and shape of the structures produced in this study.

Differential scanning calorimetry (DSC) data was obtained using the TA instruments Q20, and samples were ramped from room temperature to 300 °C at a ramp rate of 5 °C/min.

Mechanical characterization of materials was conducted using the Hysitron Triboindenter. Indentations on polymer samples were performed with a Berkovich tip and varied forces with five points per sample. A maximum drift rate of 0.1 nm/s of was set for the experiment and was automatically determined over a 40 s period. The tip was loaded to maximum load in 10 s, held for 10 s, and unloaded in 2 s. The load–depth curves were analyzed using the Oliver–Pharr model to obtain the reduced modulus (E_r) and the hardness (H) [10].

3. Results and discussion

A photo-imprint process was developed to make the high aspect-ratio, hollow-core pillars shown in Fig. 1(a). Imprint lithography may be of interest for off-chip interconnect, input/output

Author's personal copy

connections, and MEMS devices. The typical target dimensions for these applications are in the 5–200 μm range with aspect ratios ranging from 2:1 to 10:1. The photo imprint stamp shown in Fig. 1(b) was fabricated using the process flow illustrated in Fig. 4. A chrome photo-pattern was initially fabricated onto a glass substrate. To create the physical relief features, a metal seed layer was sputtered and molds for electroplating were patterned. Metal pillars were then electroplated within the photo-pattern, and the seed layer was etched back. Fig. 5 illustrates the shallow imprint process used to fabricate high aspect ratio structures, such as hollow core pillars. By using an imprint stamp with a photo-pattern and protrusions that do not transmit light, it is possible to keep a negative tone material from cross-linking in the opaque regions of the relief features in the stamp. The negative tone material can be dissolved in the unexposed regions, resulting in the selective removal of the residual layer [7,11]. Guo and coworkers noted that by using a combined imprint lithography and photolithography process, the aspect ratio of the resist patterns could be higher than the features on the stamp [7]. Since a shallow imprint process was used, a polymer layer exists between the stamp protrusions and the surface of the substrate. This polymer acts as a cushion, reducing the likelihood of the imprint stamp being damaged.

Since imprint lithography relies on mold replication to generate patterns, the imprint resist must be displaceable under elevated temperature and pressure. A pressure driving force moves the imprint resist, and capillary forces and surface energy control the wetting and spreading of the material. The simplest case in imprint lithography is that of squeeze-flow of a Newtonian fluid between two parallel disks separated by a distance corresponding to the thickness of the fluid layer. Mold filling depends on the pattern size and density, and the resist flow is governed by the viscoelastic properties of the material at the imprint temperature and pressure. The imprint material must also have sufficient mechanical strength to retain the stamp patterns after separation of the substrate from the stamp. Therefore, imprint materials are selected for their ability to replicate and retain mold patterns and for their functionality in the final application.

For thermal imprinting, the glass transition temperature (T_g) of a polymer is often used to determine the imprint temperature and the de-molding temperature [12]. Schift et al. recommended an imprint temperature 50–70 °C higher than the T_g of the polymer and a de-molding temperature 20 °C lower than the T_g [13]. Scheer et al. have shown that pressures around 100 bar and temperatures 90 °C above the polymer glass transition temperature are optimal for material displacement [14,15], but that the imprint process can be limited by poor material transport. The T_g of cured Avatrel 2000P is above 250 °C; however, the photo-imprint process requires that the polymer be imprinted before photo-patterning. Avatrel 2000P is a photosensitive dielectric that is processed at 100 °C and cured at 160 °C, and operating at temperatures much higher than the photo-processing conditions can initiate thermal cross-linking of the material. DSC analysis was conducted of soft baked films of Avatrel 2000P to assess the T_g of the material and ascertain an imprint processing window. No clear T_g could be determined from the data in Fig. 6, but it did show that the material thermally cross-links at temperatures above 150 °C.

In addition to ensuring proper material transport, minimizing adhesion between the stamp and substrate is also important in imprint lithography. Since imprint stamps have surface relief patterns, the effective total surface area that contacts the imprint material is high. Imprint material will readily adhere to stamps with no surface treatments. Adhesion between the stamp and the wafer can increase defect generation in the imprinted pattern, damage the stamp, or cause imprint material–substrate delamination. There are several strategies used to reduce adhesion between the stamp and substrate including: (i) applying a low surface

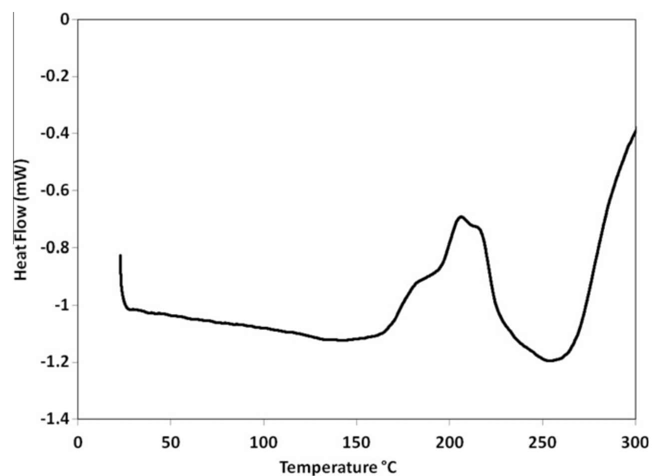

Fig. 6. DSC data of Avatrel 2000P with a ramp rate of 5 °C per min.

energy coating to the stamp, (ii) using a stamp material with an intrinsically low surface energy, and (iii) incorporating a release agent into the imprint resist formulation. A self-assembled monolayer of a fluorosilane release agent is generally solution-phase or vapor-phase deposited on the stamp surface. The silanes have low surface energy, high surface reactivity, and high resistance at elevated temperature and pressures [16]. It has also been shown that amorphous fluoropolymers such as Teflon AF can be used as an imprint release layer. The solution can be cast over the imprint stamp [17] or a flexible stamp can be made of the fluoropolymer [18].

A 7 μm photo-imprint stamp was coated with a (3,3,3-trifluoropropyl)dimethylchlorosilane anti-adhesion agent (Gelest) and imprinted into a soft baked 12 μm film of Avatrel 2000P. An operating pressure of 15 bar was initially selected, as it was the minimum operating pressure on the tool, and an imprint time of 10 s was selected to maintain high throughput. Temperature was varied and the patterns were assessed for fidelity, field planarity, and ability to separate without damaging the stamp or substrate. Below 90 °C, the imprint pattern could not be transferred in 10 s and above 115 °C, the stamp and the substrate could not be separated. The sample imprinted at 115 °C had the smallest residual flow fields around the pillar. However, Avatrel 2000P had a strong adhesion to the stamp even with the anti-adhesion agent, and its adhesiveness increased with increasing imprint temperature. As a result, more damage was caused to the stamps imprinted at 115 °C. Subsequent imprinting into Avatrel 2000P was therefore conducted at 90 °C and 15 bar for 10 s. Extended imprint times and pressures were also studied at 90 °C, but showed no appreciable improvement.

To assess the improvement in the aspect-ratio of the patterned structures, a 60 μm photo-imprint stamp was imprinted into 125 μm of soft-baked Avatrel 2000P at 90 °C, 15 bar, for 10 s. The sample was then photo-patterned in the Obducat imprint tool with an exposure dose of 200 mJ/cm^2 exposure dose. After separation, the sample was post-exposure baked for 20 min in an oven at 100 °C and ultrasonically developed in BIOACT EC-7R for 2 min. As shown in Fig. 7, the shallow 60 μm photo-imprint stamp was able to clear the full 125 μm polymer core. The structure in Fig. 7 has a center core of 104.5 mm at the top of the polymer structure. This dimension is very close to the designed size of 100 μm. Polymer dielectrics often have distorted shapes after curing due to film shrinkage or distortions from the exposure profile. In this case, the distortion of the original feature is small and an advantage to this processing approach. The center structure is fully cleared of polymer. The roughness of the inner and outer wall can be seen in the figure. As shown in Fig. 7, the roughness of

Author's personal copy

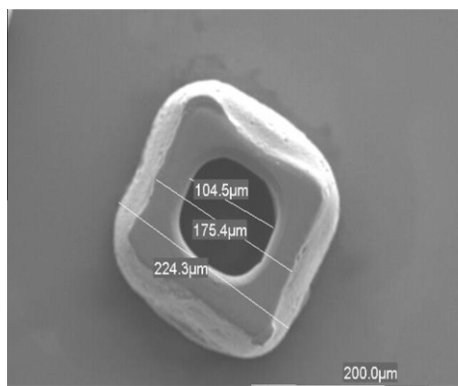

Fig. 7. Avatrel 2000P sample photo-imprinted at 90 °C, 15 bar, 10 s and an exposure dose of 200 mJ/cm^2.

the center core (the imprint region) is less than the outer boundary of the structure showing that the imprint method left the developed region smoother than the photo-patterned region.

The height-to-width ratio of the stamp was approximately 0.6, and the pattern on the substrate had a ratio of 1.25 which is more than a 2-fold increase in aspect ratio. However, the photo-pattern had poor fidelity when compared to structures made with photolithography. The Obducat imprint lithography tool has a broad band UV lamp with an intensity of 200 mW/cm^2; the high intensity makes it difficult to optimize the exposure dose for materials. Additionally, the exposure was conducted at the imprint temperature and pressure. These issues make it difficult to fairly compare the fidelity of the photo-imprint process in Fig. 7 with a structure patterned with photolithography.

Avatrel 8000P was used to evaluate how the photo-imprint lithography process compares with optical resolution capabilities for high aspect ratio structures. A feature set that could not be fabricated with optical lithography was characterized and then tested with the photo-imprint lithography process. The free standing, hollow core pillars shown in Fig. 1(a) were first attempted using photolithography. A film of Avatrel 8000P was spin coated to a thickness of approximately 30 µm onto a silicon oxide coated wafer and soft baked at 100 °C for 5 min on a hotplate. Features with a 10 µm core diameter and a total diameter of 30 µm were exposed to doses of 500, 400, and 300 mJ/cm^2 and developed using two different techniques. An optical dissolution rate monitor was used to evaluate the optimal development time for the Avatrel 8000P samples. However, the material became very rough during development making the thickness difficult to quantify during dissolution. To establish a minimum development time, films of Avatrel 8000P were spin coated, soft baked, and puddle developed. The unpatterned film dissolved completely in MF-319 in 2 min and 15 s. The photo-patterned samples were developed for 2 min and 30 s since significant delamination of features occurred with longer development times.

The profile data of the features is summarized in Table 1; a height of zero represents the wafer/polymer interface and a height of approximately 28 µm represents the top of the film. At an exposure dose of 500 mJ/cm^2, the core height is 24.85 µm suggesting that only about 3 µm of material developed from the core. For an exposure dose of 400 mJ/cm^2, the core height was 17.67 µm suggesting that about 10 µm of material developed. The decrease in core height with a decrease in exposure dose suggests that at 500 mJ/cm^2 there is scattering within the core that hinders development of the feature. However, lowering the dose to values less than 300 mJ/cm^2 did not decrease the height of material in the core appreciably. Therefore, an alternative development technique using ultra-sonication, was used with Avatrel 8000P at an exposure dose of 400 mJ/cm^2. Samples developed in the ultra-sonic bath, had a height of 15.03 µm suggesting that transport of the developer within the core does impact the ability to pattern the structure.

Table 1
Height profiles for varying exposure and development times with Avatrel 8000P.

Dose (mJ/cm^2)	Develop type	Time (min:s)	Core height (µm)
500	Puddle	2:30	24.85 ± 0.47
400	Puddle	2:30	17.67 ± 0.19
400	Ultrasonic	2:30	15.03 ± 0.12
300	Puddle	2:30	17.37 ± 0.31

The photo-imprint stamp fabrication process flow is illustrated in Fig. 4. A glass wafer was sputtered with chrome and then photo-patterned to have the same photo-pattern as the photo-mask used in photolithography. Copper pillars were electroplated in the center of the collar to physically displace material during imprint and also eliminate the need for alignment. Since the photo-imprint stamp has a high density of protrusions on its surface, it has a high total surface area in contact with the imprinted polymer which makes it possible for the polymer to adhere to the stamp. (3,3,3-Trifluoropropyl)dimethylchlorosilane, was used as the anti-stick layer in this application. Researchers have noted that fluorosilane layers applied to UV imprint stamps have been shown to be attacked by different photosensitive materials [19]. Therefore, Teflon AF was used as an anti-reflective and mold release coating. The material has excellent light transmission from the deep UV range out through visible spectrum, and because it does not absorb light, it will not deteriorate with exposure to light [20].

DSC analysis of the soft-baked Avatrel 8000P film was used to determine the processing window for the material, as shown in Fig. 8. There is a slight inflection in the graph around 70 °C, and the material begins thermally cross-linking at approximately 140 °C. To determine the optimal temperature for imprint, a stamp with 15–16 µm tall copper pillars was imprinted into a 30 µm film of Avatrel 8000P at 45 bar for 60 s for incremental temperatures shown in Fig. 9. Imprinting at 150 °C displaced the full height of the stamp; however, imprinting at this condition also initiated thermal cross-linking of the material, which inhibited subsequent photo-patterning of structures. Imprinting at 125 °C, 45 bar for 60 s, did not displace the full height of the stamp, and increasing time or pressure did not cause the stamp to displace its full height. Due to viscous polymer flow, the large-scale protrusion patterns cannot fully penetrate the polymer yielding a reduced aspect ratio

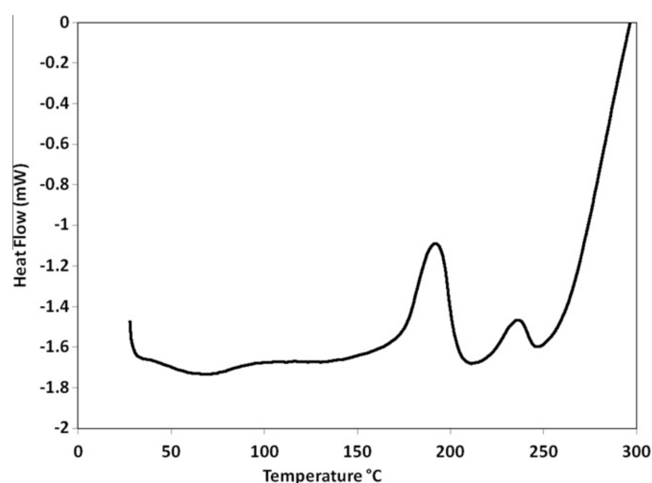

Fig. 8. DSC data of Avatrel 8000P with a ramp rate of 5 °C per min.

Author's personal copy

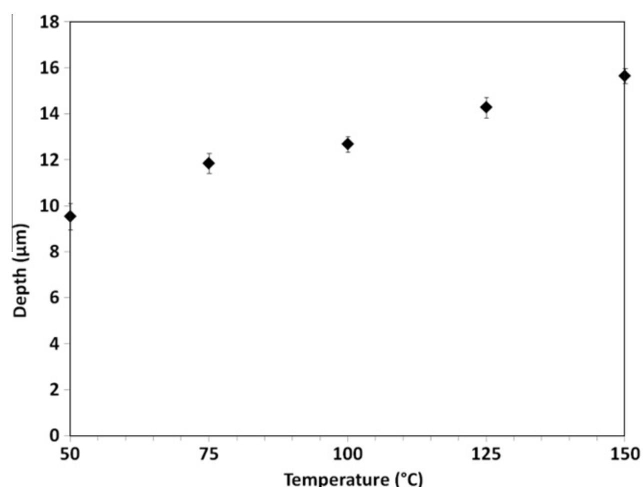

Fig. 9. Depth vs. temperature for thermal imprinting into Avatrel 8000P at 45 bar and 60 s.

than intended [11]. However, thermal cross-linking of the material was not initiated at this temperature; consequently, subsequent imprints were conducted at 125 °C, 45 bar for 60 s.

To evaluate the impact of incomplete pattern transfer on field planarity, a non-contact profilometer was used to profile the height around the features, immediately after imprinting, but before photo-patterning the sample. The depth profiles were averaged for 10 similar features using the profilometer software. A cross-sectional view of the feature is shown in Fig. 10 for the averaged data. Zero refers to the top of the film in Fig. 10, and the material displaced by the copper pillar appears to buildup around the perimeter of the feature. Examination of the data suggests that approximately 0.5 µm of non-planarity exists around the imprinted feature. The non-contact profilometer uses the phase change of light reflecting from various heights of similar materials to measure the uniformity of a flat surface or the horizontal distance between two adjacent surfaces. There is little sidewall profile data since light that reflects from the sidewalls is not captured by the sensor.

To compare the performance of photo-imprinting with photolithography, Avatrel 8000P samples were imprinted in the tool at 125 °C, 45 bar for 60 s and then exposed in the Karl Suss MA-6 Mask Aligner. After separation, the samples were puddle developed for 2.5 min. The height of the imprinted pattern is shown in Fig. 11. The black region in this plane-view refers to the silicon oxide substrate and the grey refers to the top of the feature. The core of the pillar is also black suggesting that the pillar has been fully developed. A two dimensional height analysis was also conducted of the feature to confirm that the core had cleared, and a cross-section of the feature is shown in Fig. 12. The photo-imprint process was able to fully develop the hollow core pillar with a (height to width) aspect ratio of 2.8 which was not possible with photolithography. The fidelity of the imprinted feature is excellent; Fig. 12 shows a hole very close to the 10 µm design target dimension. The photo-imprint process reduced scattering within the core and also facilitated development within the core by displacing material.

Imprint lithography demonstrated the ability to enhance the photo-patterning of polymer dielectrics such as Avatrel 2000P and Avatrel 8000P. Avatrel 2000P and Avatrel 8000P both have polynorbornene backbones, but have different optical, mechanical, and electrical properties [9,21,22]. The mechanical properties of Avatrel 2000P and Avatrel 8000P were evaluated to assess their impact on imprinting. A brief mechanical comparison of Avatrel 2000P and Avatrel 8000P after cure was conducted with nano-indentation. Avatrel 2000P is a softer material with a modulus of 1.0 GPa and hardness of 0.04 GPa, whereas Avatrel 8000P has a modulus value of 2.9 GPa and hardness of 0.18 GPa.

To evaluate the mechanical properties of the soft-baked materials, nano-indentation of both materials was conducted at a force of 1000 µN and the load vs. displacement is shown in Fig. 13. The modulus and hardness of Avatrel 2000P after soft-bake were 0.46 and 0.01 GPa, respectively, and the modulus and hardness of Avatrel 8000P after soft-bake were 1.1 and 0.04 GPa, respectively. As a result, for a given force the photo-imprint stamp displaces a greater distance in Avatrel 2000P than in Avatrel 8000P. The same photo-imprint stamp imprinted into Avatrel 8000P was imprinted into a 30 µm film of Avatrel 2000P at 45 bar for 60 s for incremental temperatures from 50 to 125 °C. The full height of the stamp was displaced at 50 °C for Avatrel 2000P, whereas the full height of the stamp was only displaced at 150 °C for Avatrel 8000P. Avatrel 8000P is four times harder than Avatrel 2000P and therefore, required much higher imprint temperatures. As shown by the DSC data, imprint temperatures are limited for photo-sensitive materials by thermal cross-linking. Higher imprint pressures and longer imprint times can compensate for the limited temperature processing window. As demonstrated, a 7 µm stamp was able to

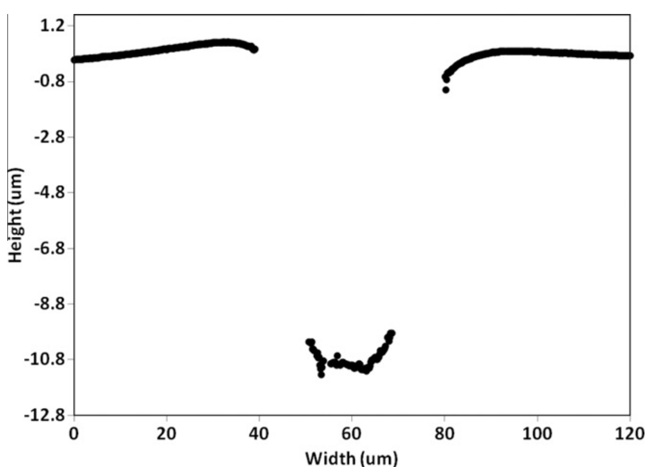

Fig. 10. Non-contact optical depth profile of thermal imprint Avatrel 8000P sample at 125 °C, 45 bar, and 60 s.

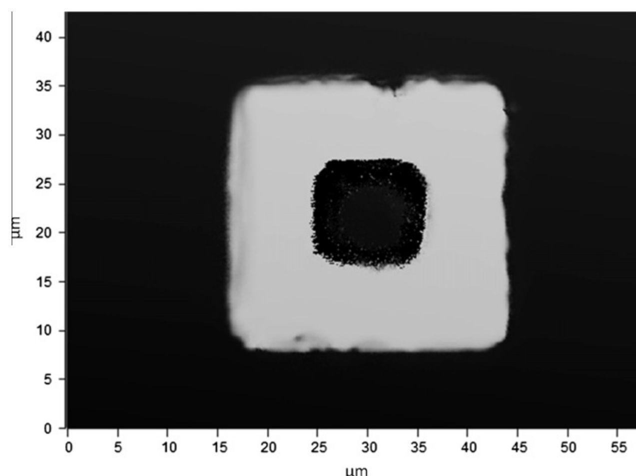

Fig. 11. Grey-scale map of the height of the photo-imprinted feature into Avatrel 8000P at 125 °C, 15 bar, 60 s, exposure dose of 500 mJ/cm^2 and puddle develop for 2 min 30 s.

Author's personal copy

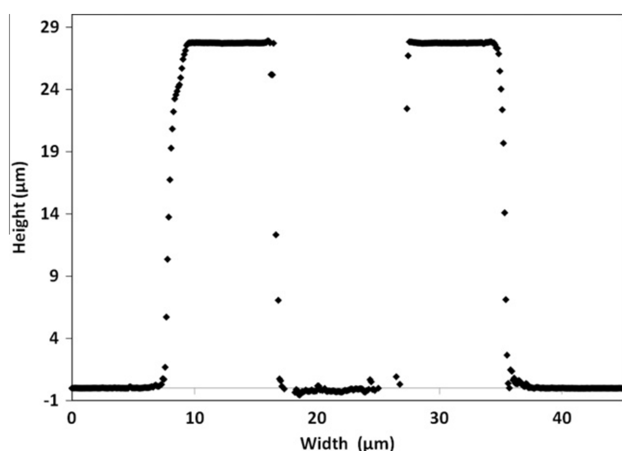

Fig. 12. Two dimensional height profile of the photo-imprinted feature into Avatrel 8000P at 125 °C, 15 bar, 60 s, exposure dose of 500 mJ/cm^2 and puddle develop for 2 min 30 s.

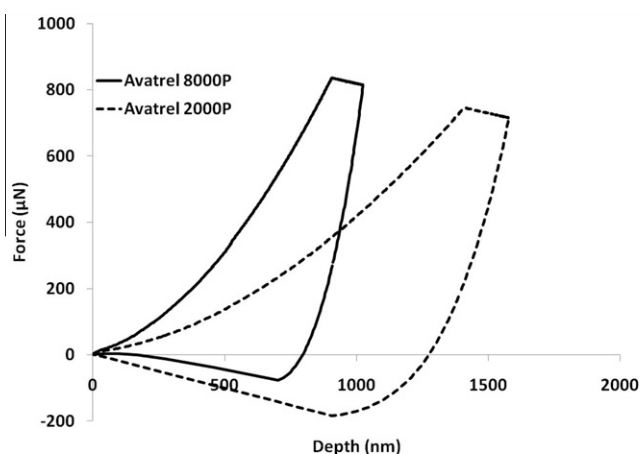

Fig. 13. Force vs. displacement curves with a maximum force of 1000 µN for Avatrel 8000P (solid line) and Avatrel 2000P (dashed line) after soft-bake.

Table 2
Height profiles of non-planarity of Avatrel 2000P and Avatrel 8000P imprint samples at 45 bar, 60 s and varying temperatures.

Temperature (°C)	Avatrel 2000P Height (µm)	Avatrel 8000P Height (µm)
50.00	0.18	0.79
75.00	0.24	0.98
100.00	0.20	0.71
125.00	0.11	0.50

imprint Avatrel 2000P at 90 °C, 15 bar, and 10 s, and a 15 µm stamp was able to imprint Avatrel 2000P at 50 °C, 45 bar, and 60 s. A much taller stamp was able to imprint at a lower temperature in Avatrel 2000P due to the increased imprint pressure and time. Due to the processing limitations of the imprint tool, pressure could not be elevated sufficiently to transfer the full 15 µm height of the stamp in Avatrel 8000P at temperatures below its thermal crosslink temperature.

The non-planarity of Avatrel 2000P and Avatrel 8000P over the range of temperatures was also compared, and the data is presented in Table 2. A non-contact profilometer was used to map the height of material buildup around the perimeter of the imprinted features as shown in Fig. 10. For each temperature, the height profiles were averaged for 10 similar features using the profilometer software and zero was set to the height of the film in the field. The non-planarity around the features varies at the lower temperatures, but both Avatrel 2000P and Avatrel 8000P had the lowest measured non-planarity around the imprinted feature at a temperature of 125 °C. Avatrel 2000P also consistently displayed a greater level of planarity than Avatrel 8000P. Longer times and higher pressures were attempted, but significant improvement in field planarity was not achieved. Elevating the imprint temperature made the largest impact on field planarity, but the imprint temperature was limited due to the susceptibility of the materials to initiate thermal cross-linking.

Photo-imprint lithography requires the optimization of material properties for both thermal imprinting and photo-patterning. The lower modulus material, Avatrel 2000P, could be imprinted at lower temperatures, pressures, and times; it also had lower levels of non-planarity. Avatrel 8000P when imprinted had an incomplete stamp pattern transfer which reduced the aspect ratio of the imprinted structures. However, complete filling was not critical for this application since photo-patterning eliminated the residual flow fields, and Avatrel 8000P has the photo-definition capability to produce high aspect ratio structures. A summary of results is presented in Table 3.

Table 3
Imprint results achieved in this study for Avatrel 2000P and 8000P.

	Avatrel 2000P	Avatrel 8000P
Soft-baked modulus (GPa)	0.46	1.1
Soft-baked hardness (GPa)	0.01	0.04
Optimized imprint conditions	90 °C, 15 bar, for 10 s	125 °C, 45 bar for 60 s
Non-planarity at imprint condition (µm)	0.2	0.5
Aspect ratio with photo-imprint process (h:w)	1.25:1	2.8:1
Improvement over photo-lithography	2.5×	1.8×

4. Conclusion

A novel fabrication method has been developed to enhance the photo-patterning of polymer dielectrics for high aspect ratio hollow structures. The photo-imprint stamp was able to physically move material in the polymer core and reduce the effective film thickness compared to the bulk film. The reduction in film height reduced the effects of scattering in the core and also facilitated transport of developer within the core. The integrated photo-imprint lithography process fabricated high aspect ratio hollow core pillars that exceeded the resolution of the imprint stamp and optical resolution. This process was tested with Avatrel 2000P and Avatrel 8000P which are polymer dielectrics with different mechanical and photo-patterning properties. Photo-imprint lithography requires balancing mechanical properties that are suitable for thermoplastic imprinting and photo-definition properties for subsequent photo-patterning.

Acknowledgements

The authors gratefully acknowledge the support of the Interconnect Focus Center, one of six Focus Centers. The authors also acknowledge the support of Promerus LLC for providing materials for this research and many useful discussions.

Author's personal copy

References

[1] S.Y. Chou, P.R. Krauss, P.J. Renstrom, Applied Physics Letters 67 (1995) 3114–3116.
[2] S.Y. Chou, P.R. Krauss, P.J. Renstrom, Journal of Vacuum Science & Technology B 14 (1996) 4129–4133.
[3] S.Y. Chou, P.R. Krauss, L. Kong, Journal of Applied Physics 79 (1996) 6101–6106.
[4] S. Chou, P. Krauss, P. Renstrom, Science 272 (1996) 85.
[5] S. Chou, P. Krauss, W. Zhang, L. Guo, L. Zhuang, Journal of Vacuum Science and Technology-Section B-Microelectronics Nanometer Structure 15 (1997) 2897–2904.
[6] D. Resnick, W. Dauksher, D. Mancini, K. Nordquist, E. Ainley, K. Gehoski, J. Baker, T. Bailey, B. Choi, S. Johnson, Journal of Microlithography, Microfabrication, and Microsystems 1 (2002) 284.
[7] X. Cheng, L. Jay Guo, Microelectronic Engineering 71 (2004) 288–293.
[8] R. Tummala, Fundamentals of Microsystems Packaging, McGraw-Hill Professional, 2001.
[9] V. Rajarathinam, C. Lightsey, T. Osborn, B. Knapp, E. Elce, S.A.B. Allen, P.A. Kohl, Journal of Electronic Materials 38 (2009) 778–786.
[10] W. Oliver, G. Pharr, Journal of Materials Research 7 (1992) 1564–1583.
[11] X. Cheng, L. Jay Guo, Microelectronic Engineering 71 (2004) 277–282.
[12] H. Schift, L.J. Heyderman, in: D.J. Lockwood (Ed.), Nanostructure Science and Technology, Kluwer, Academic, New York, 2003, pp. 46–76.
[13] H. Schift, S. Bellini, J. Gobrecht, F. Reuther, M. Kubenz, M. Mikkelsen, K. Vogelsang, Microelectronic Engineering 84 (2007) 932–936.
[14] H. Schulz, H. Scheer, T. Hoffmann, C. Torres, K. Pfeiffer, G. Bleidiessel, G. Grützner, C. Cardinaud, F. Gaboriau, M. Peignon, Journal of Vacuum Science & Technology B: Microelectronics and Nanometer Structures 18 (2000) 1861.
[15] H. Scheer, H. Schulz, T. Hoffmann, C. Torres, Journal of Vacuum Science & Technology B: Microelectronics and Nanometer Structures 16 (1998) 3917.
[16] H. Schift, S. Saxer, S. Park, C. Padeste, U. Pieles, J. Gobrecht, Nanotechnology 16 (2005) 171.
[17] D. Khang, H. Khang, T. Kim, H. Lee, Nano Letters 4 (2004) 633–637.
[18] D. Khang, H. Lee, Langmuir 20 (2004) 2445–2448.
[19] F. Houle, C. Rettner, D. Miller, R. Sooriyakumaran, Applied Physics Letters 90 (2007) 213103.
[20] DuPont. Teflon® AF Properties. 2010; Available from: <http://www2.dupont.com/Teflon_Industrial/en_US/products/product_by_name/teflon_af/properties.html>.
[21] Y.Q. Bai, P. Chiniwalla, E. Elce, R.A. Shick, J. Sperk, S.A.B. Allen, P.A. Kohl, Journal of Applied Polymer Science 91 (2004) 3023–3030.
[22] Y.Q. Bai, P. Chiniwalla, E. Elce, S.A.B. Allen, P.A. Kohl, Journal of Applied Polymer Science 91 (2004) 3031–3039.